Journal of Cleaner Production 515 (2025) 145759

Contents lists available at ScienceDirect

Journal of Cleaner Production

journal homepage: www.elsevier.com/locate/jclepro

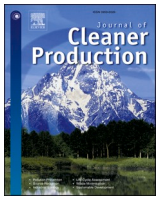

Recyclable polyester textile waste-based composites for building applications in a circular economy framework

José Carlos Ferreira Junior [a,b], Ennouri Triki [b], Olivier Doutres [a], Nicole R. Demarquette [a], Lucas A. Hof [a,*]

[a] Department of Mechanical Engineering, École de Technologie Supérieure, 1100, Rue Notre-dame Ouest, Montreal, Québec, H3C 1K3, Canada
[b] Apparel Research and Innovation Center, Vestechpro, 7000 Marie-Victorin Street, Montreal, H1G 2J6, Canada

ARTICLE INFO

Keywords:
Sustainable composites
Circular economy
Recyclable
Eco-friendly building materials
Polyester textile waste
Insulation panels

ABSTRACT

There is a growing need for sustainable solutions to address the increasing levels of textile waste at both post-industrial and post-consumer stages. Easily implementable solutions could accelerate adoption in circular economy applications. In this context, post-industrial polyester and a water-soluble adhesive were combined to fabricate recyclable textile-based composite panels using a room-temperature processing method, reinforcing sustainable practices by lowering energy demands and material use. The resulting composites exhibited tunable acoustic performance: increased textile content enhanced sound absorption but introduced higher porosity during fabrication, which affects the material's overall performance. Additionally, the composites displayed a low thermal conductivity of 0.05 W/m·K, making them suitable for energy-efficient insulation applications, and enhanced toughness, with optimal flexural toughness at 37 wt% and impact toughness at 52 wt% textile content. The ability to recover the materials at room temperature using water demonstrates a simple and effective recycling process, further extends their lifespan, highlighting their potential for resource-efficient reuse within a circular economy framework. These recyclable composites can be directly applied in building construction, offering a sustainable alternative for applications such as insulation panels, acoustic treatments, and non-structural building components. This research advances efforts toward resource-conscious and sustainable production by reducing textile waste and promoting the circular reuse of materials in the construction industry.

1. Introduction

While clothing is essential to daily life, its production and disposal are part of a far more complex environmental issue. The textile and clothing industries are among the world's most polluting sectors (Mandarić et al., 2022), (Nørup et al., 2018) responsible for 8–10 % of global CO_2 emissions (Leal Filho et al., 2022), with fast fashion being one contributing factor (Niinimäki et al., 2020). This business model supports a disposable clothing trend (Caro et al., 2015), (Yang et al., 2017), where retail consumers are incentivized to overconsume fashionable items at a lower price (Brewer, 2019), (Casais and Faria, 2022). Consequently, higher consumption and overproduction result in greater environmental burdens, including over 92 million tonnes being sent to landfills or incinerated each year (Niinimäki et al., 2020). This includes polyester, the most common fiber in textiles, a synthetic fiber derived from a non-renewable resource (Ellen MacArthur Foundation, 2017). As a non-biodegradable material, polyester persists in the environment for extended periods (Egan and Salmon, 2022), contributing to microplastic pollution. These microplastics are released into the atmosphere during use, such as laundering and wear (Nayanathara Thathsarani Pilapitiya and Ratnayake, 2024) or disposed, and accumulate in terrestrial and aquatic ecosystems (Dris et al., 2016), further intensifying the problem. Only a small fraction of the textile waste is effectively processed at the end of its lifecycle. In the US and EU, these figures are estimated to be 15 % and 26 %, respectively (Bukhari et al., 2018), (Juanga-Labayen et al., 2022). As a result, most of this waste is disposed of in landfills or incinerated (Shirvanimoghaddam et al., 2020), representing a significant and preventable environmental concern. This current scenario highlights the need to explore this waste stream, prioritizing sustainable practices over linear disposal methods (Delpla et al., 2022), (Delbari and Hof, 2024).

Addressing textile waste requires a focus on reducing future waste

* Corresponding author.
E-mail addresses: jose-carlos.ferreira-junior@etsmtl.ca (J.C. Ferreira Junior), triki.ennouri@gatineau.ca (E. Triki), olivier.doutres@etsmtl.ca (O. Doutres), nicoler.demarquette@etsmtl.ca (N.R. Demarquette), lucas.hof@etsmtl.ca (L.A. Hof).

https://doi.org/10.1016/j.jclepro.2025.145759
Received 29 January 2025; Received in revised form 25 April 2025; Accepted 18 May 2025
Available online 20 May 2025

generation and developing possible solutions for its use (Yalcin-Enis et al., 2019). For example, consumers, given proper instruction, would be able to assess more accurately their clothing purchases, waste decisions and extending clothing lifespans through reuse, reducing their environmental impact (Nørup et al., 2018). This is particularly relevant given that, at least in wealthy countries, most of the textiles in the residential waste stream were prematurely discarded, being still good for reuse (Farrant et al., 2010), (Nørup et al., 2019), a finding corroborated by research conducted in Canada (Drennan et al., 2021). Simultaneously, addressing the existing stockpiles of textile waste is also essential. Recycling has been used to handle current waste as a possible solution.

Textile recycling routes are usually grouped by processing technique, either mechanical or chemical. The former involves the mechanical separation of textiles, and the latter involves their dissolution or depolymerization. Alternatively, considering that multiple processing techniques may be used during recycling, Sandin et al. (Sandin and Peters, 2018) proposed a classification based on the type of recycled material recovered, namely, fabric, fiber, polymer, and monomer (Sandin and Peters, 2018). This classification provides a more practical approach to the application of recycled materials and their development in different applications. Given this perspective and the simplicity of achieving the recycled stage of fabric and fibers by means of mechanical recycling, it is reasonable to explore their potential applications. The existing literature on the applications of recycled fabrics or fibers can be broadly categorized into different groups as follows (Fig. 1): A. Composites, including A1. fillers (DeVallance et al., 2012), A2. reinforcement (Chen et al., 2021), (Petrucci et al., 2015), (Ramamoorthy et al., 2014), A3. preforms (Frydrych et al., 2018), (Mishra et al., 2014), and A4. bio-based composites (Lacoste et al., 2018), (Ramamoorthy et al., 2018), (Temmink et al., 2018), (Huang et al., 2024); B. Geotextiles, such as B1. kemafil rope (Broda et al., 2019) and B2. soil reinforcement (Rahman et al., 2021). C. construction materials, including, C1. concrete reinforcement (Wang, 1999), C2. panels (DeVallance et al., 2012), (Barbero-Barrera et al., 2016), C3. lightweight bricks (Algin and Turgut, 2008), C4. polymer concrete (Peña-Pichardo et al., 2018), C5. flooring (Echeverria et al., 2019), and C6. non-structural (DeVallance et al., 2012), (Echeverria et al., 2019), (Sadrolodabaee et al., 2021a), (Sadrolodabaee et al., 2021b), (Sadrolodabaee et al., 2021c). D. Insulation, such as D1. thermal (Briga-Sá et al., 2013), D2. sound (Echeverria et al., 2019), (Pegoretti et al., 2014), or D3. both (Dissanayake et al., 2018), (Patnaik et al., 2015). E. Others, such as E1. heavy metal adsorbents (Bediako et al., 2016), E2. footwear (Fernandes et al., 2021) and E3. mattress filing (Nayak et al., 2020). The list of applications is far from extensive, but it demonstrates that while propositions are not new, they have become more prevalent in recent years. Approximately 81 % of those studies were published in the last decade, with the fields of construction and composites accounting for around 70 % of the applications.

Previous studies provide valuable insight into the potential applications of recycled textile materials, but the complexity of manufacturing processes can hinder their development. Prioritizing simpler processes, especially in regions with large waste streams, can significantly enhance their viability, scalability, and accessibility (Kunlere and Shah, 2023), (Pajunen et al., 2016). Barbanera et al. (2020) offer a practical example of this approach by demonstrating the feasibility of producing building insulation materials using a straightforward technique: simply compression molding leather scraps with polyvinyl acetate (PVAc) as a binder, followed by consolidation in an oven at 70 °C (Barbanera et al., 2020). This simplicity serves as an important step in improving the usage of diverse waste streams, shifting the emphasis away from individual fiber properties, a key factor in closed-loop recycling, and instead prioritizing bulk material properties, which enable more flexible and open-ended recycling based applications (Drennan et al., 2021), (Sandin and Peters, 2018). For instance, Dissanayake et al. (2018) sandwiched shredded pieces of apparel industry waste using hot pressing at 215 °C for thermal insulation applications (Dissanayake et al., 2018). Building upon these findings, which demonstrated successful consolidation at higher temperatures, future research could direct attention to room-temperature methods. This shift could enhance the viability of these simplified processes for greater practical application.

To expand the range of sustainable building materials and offer a viable solution for textile waste, this study aimed to explore a simple, room-temperature fabrication process for textile waste composites using

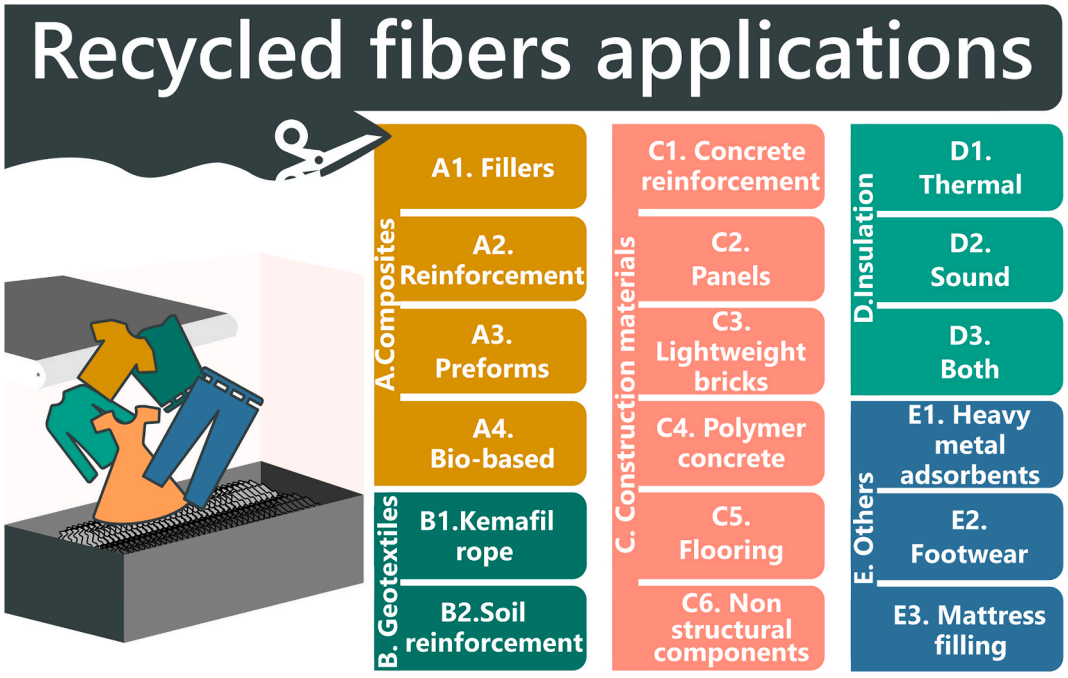

Fig. 1. Recycled textile fiber applications available in the literature.

widely available materials for building applications. Post-industrial shredded polyester, in varying weight percentages, was manually combined with PVAc, a common binding agent for nonwovens in the textile industry (Petrucci et al., 2015), at room temperature. By characterizing the morphology, mechanical properties, thermal and acoustic performance of the resulting composite panels, as well as their recyclability, this research provides a simple solution for transforming textile waste into a more sustainable building material for thermal insulation, tunable acoustic properties, or others non-structural applications. To the best of our knowledge, this research is the first to demonstrate a room-temperature process that incorporates a straightforward water-based recycling method for textile waste, distinguishing it from other approaches. It also offers insights to support further exploration of recyclable composites for broader applications, thereby extending the lifespan of textile waste.

2. Materials and methods

The following section outlines the materials and experimental procedures used in this study.

2.1. Materials

A mix of post-industrial polyester waste fabrics, primarily offcuts with irregular shapes from industrial production (dimensions ranging from 20 to 50 cm × 20–50 cm), was employed. A commercially available adhesive of polyvinyl acetate (PVAc) water dispersion (Henkel, Canada) was used as received. After water evaporation an average solid content of 45.8 wt% for PVAc was determined from a triplicate measurement and it was used to produce the composite panels at different weight contents. An acrylonitrile butadiene styrene (ABS) filament (Ultimaker) for fused deposition modeling (FDM) 3D printing was utilized to produce the mold for the textile panels.

2.2. Methods

2.2.1. Mechanical transformation of textile

A fabric shredder SF-2CA (IPEA) equipment was used to mechanically transform the post-industrial polyester textile fabrics. The fabric was cut into smaller pieces (ranging from 10 to 25 cm × 10–25 cm) to allow for easier feeding into the equipment. The fabric was placed in an infeed belt conveyor where a feeder roller transported it to a shredding cylinder, reducing the textile material to a combination of three different levels, fabric, yarn, and fibers (Fig. 2). The obtained materials were reprocessed for a total of four times, until a more homogeneous combination of yarn and fabric was obtained.

2.2.2. Mold and panels fabrication

In order to produce the textile panels 3D printed molds pieces were made using an Ultimaker S5 (Ultimaker), a FDM 3D printer. Shredded material was manually combined with adhesive, adding water as needed to facilitate mixing. This mixture was then fed into the mold and subjected to a pressure of 815 N for 24 h. The panel was left to dry and consolidate in open air at room temperature (20–25 °C). Fig. 2 provides a schematic illustration of the process.

Textile panels with 13 × 18.5 cm and thicknesses varying between 2 and 3.5 cm were produced. A total of four different compositions containing 40, 50, 60 and 65 wt% of recycled textiles were obtained. After final consolidation the composites with recycled textile material contained 37, 52, 60 and 63 wt% with a random orientation. To evaluate the effect of textile addition in comparison to the adhesive alone, control samples were prepared using adhesive only. These control samples were produced by pouring 200 g of adhesive into a rectangular silicone mold and curing it at room temperature (RT) in a fume hood for three weeks. Additionally, the fabricated samples were prepared for additional testing as required, by operations of cutting and sanding to create a flatter surface when needed.

2.2.3. Characterization

Table 1 presents a simplified overview of the materials characterization performed, categorized by the investigated properties. The different techniques used by material type are indicated with a check mark. A detailed description of each characterization technique is presented next.

2.2.3.1. Morphology. The textile material before and after mechanical transformation, cross-section of the adhesive, the surface of the composites and the fractured region of mechanically tested composites were observed with a scanning electron microscope (SEM) Hitachi MEB-3600-N at an accelerating voltage of 5 kV. Samples were gold coated using an

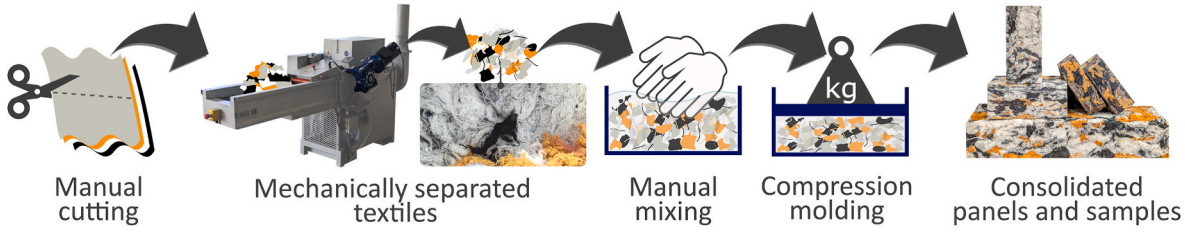

Fig. 2. Schematic illustration of the fabrication process from fabric to textile composite panels.

Table 1
Overview of the investigated materials properties.

Investigated Property		Materials							
		Adhesive	Textile			Composites (wt.%)			
			Fibers	Yarn	Fabric	37	52	60	63
Surface	**Morphology**	✓	✓	✓	✓	✓	✓	✓	✓
Physical	**Density**	✓	✓	–	–	✓	✓	✓	✓
	Contact Angle	✓	✓	–	–	✓	✓	✓	✓
	Thermal Conductivity	✓	–	–	–	✓	✓	✓	✓
	Acoustic	–	–	–	–	✓	✓	✓	✓
Mechanical	**Flexural**	✓	–	–	–	✓	✓	✓	✓
	Impact	–	–	–	–	✓	✓	–	–
Recyclability	**Materials recovery**	–	–	–	–	–	–	–	✓

Emitech K550X sputter coater. For the mechanically transformed textiles three samples were investigated a piece of fabric, yarn and fiber, randomly selected. They were also observed under transmitted light using an Olympus BX51 optical microscope equipped with an OptixCam Summit SK2-5.2X digital camera.

2.2.3.2. Density and percentage of porosity. Density (ρ) measurements were conducted with the help of an AccuPyc II 1340 gas pycnometer using helium to determine the sample volume. A 35 cm^2 cup was used as a container to perform the measurements of the composite panels and the adhesive. A cycle of 10 purges followed by 10 volumetric measurements was performed, with the average density based on the average volume and mass of the sample, weighted prior to testing. The percentage of porosity (ϕ) was determined based on the bulky density (ρ_b) of the samples and their density using Equation (1):

$$\phi = \left(1 - \frac{\rho_b}{\rho}\right) \times 100 \quad \text{Eq. 1}$$

bulk density was determined based on the total mass and volume of the samples, with the dimensions measured using a caliper.

2.2.3.3. Contact angle. The wettability of the materials under study were evaluated through contact angle measurements with water. These measurements were performed on the surfaces of adhesives, textile panels, and mechanically transformed textiles in the form of loose fibers, which were randomly selected. A VCA Optima goniometer was used to perform the measurements with ultrapure water at RT. The images were taken just after the drop was deposited on the surface of the material; a total of 5–6 measurements were conducted for each sample. The contact angle was calculated based on the average angle value between the left and right of the water droplets and material surfaces, determined using ImageJ software.

2.2.3.4. Thermal conductivity. The thermal conductivity was measured using a C-Therm Trident system. Samples were placed in a modified transient plane source sensor and held in place with a 500-g weight with no liquid contact. Five measurements were taken for each sample, with samples tested in duplicate. The inability to machine a sufficiently flat surface hindered the testing of the composites containing 63 wt% of textiles.

2.2.3.5. Acoustic properties. The acoustic properties were assessed using a commercial impedance tube (Mecanum, Sherbrooke, Canada), focusing on the measurement of the normal incidence sound absorption coefficient (SAC) and sound transmission loss (STL) of the composite panels. Cylindrical samples with varying textile content and with a diameter of approximately 44 mm and thicknesses of around 7.4 mm were prepared and tested across a frequency range of 115 Hz–4323 Hz. The SAC was measured in accordance with ASTM E1050-19 (ASTM E1050-19, 2019), considering two different mounting conditions: (1) with the samples placed directly on a rigid backing, and (2) with the samples placed on a 50 mm thick air plenum. The addition of an air cavity behind the sample provides a more realistic scenario, as potential applications for such composite panels include uses like ceiling tiles. The STL was determined from pressure measurements at three positions within the impedance tube according to the "three-microphone method" (Salissou et al., 2012) and standard ASTM E2611-09 (ASTM E2611-09, 2009). Small plastic rings and petroleum jelly were used to prevent acoustic leaks around the edges of the samples. Although only one sample per material type was evaluated, multiple measurements were performed for each acoustic indicator (SAC and STL) to identify the measurement variability associated with mounting and dismounting the samples in the tube.

2.2.3.6. Three-point bending. The flexural properties were evaluated using a three-point bending test performed on a MTS universal testing machine with a 10 kN load cell. Samples with variable thickness were placed between the supports with a 100-mm span. A test rate of 30 mm/min was used to determine the maximum flexural stress (σ_f) and the modulus of elasticity (E_B) using Equations (2) and (3):

$$\sigma_f = \frac{3FL}{2bt^2} \quad \text{Eq. 2}$$

$$E_B = \frac{L^3 m}{4bt^3} \quad \text{Eq. 3}$$

where F is the applied force (N), L is the support span (mm), b is the sample width (mm), t is the sample thickness (mm), m is the initial slope of the load–displacement curve (N/mm) (Alshahrani and Ahmed, 2021). Toughness was calculated by integrating the stress-strain curve. The final value was calculated by averaging the response of a triplicate set of samples.

2.2.3.7. Impact testing. A drop tower test machine (Cadex twin-wire) equipped with a load cell (max. 22 kN) was used to determine the samples' response under dynamic compressive solicitation during impact testing. A flying arm with a flat surface and a mass of 5 kg was used as a free fall impactor dropped from different drop heights. Two different sample compositions were tested: 37 wt% and 52 wt% of recycled material. For both compositions, drop heights were tested in 10 cm increments. Samples containing 37 wt% of recycled material were tested at heights of 10 and 20 cm, while those with 52 wt% were tested at heights ranging from 10 to 30 cm. All tested samples had a length-to-thickness ratio of at least 2 (Miltz and Ramon, 1990) and were fixed with double-sided tape to the load cell assembly. The displacement of the impactor was determined using a high-speed camera (Fastcam SA3 model 60K-M2) at 4000 Hz by tracking the markers placed on the impactor with digital image correlation. To describe the energy dissipation, two parameters were used: the coefficient of restitution (COR) and ideality (Eq. (4)). The COR, representing the ratio of the impactor's velocity before and after impact, was determined directly from the high-speed camera data. Ideality, on the other hand, required calculating the energy absorbed during compression. This was achieved by

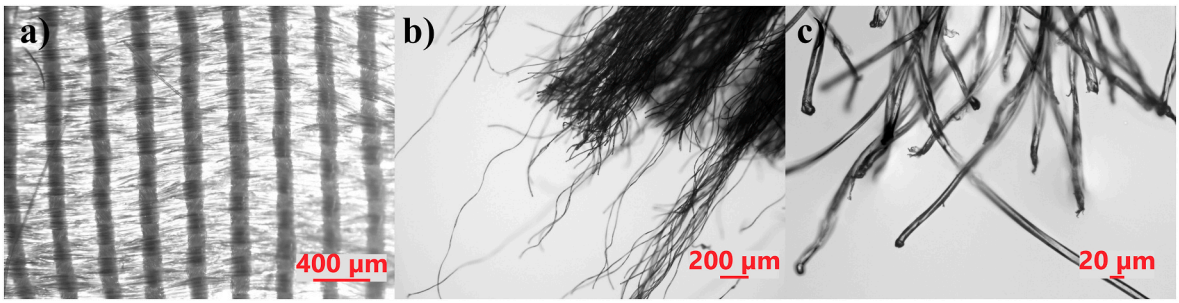

Fig. 3. Morphology of a) fabric, b) yarn, and c) fibers after mechanical transformation using OM.

first obtaining the compressive stress (σ) as a function of strain (ϵ) from the force, time, impactor displacement, and sample dimensions, as detailed elsewhere (Bailly et al., 2020). With the stress-strain data, ideality was then calculated using Equation (4) (Miltz and Ramon, 1990):

$$Ideality\ (\%) = \frac{\int_0^{\epsilon} \sigma d\epsilon}{\sigma_m \epsilon_m} \quad \text{Eq. 4}$$

where the *Ideality* (%) parameter expresses the ratio of the absorbed energy of the investigated samples to that of an ideal absorber. The maximum obtained compressive stress (σ_m) and strain (ϵ_m) of each tested drop height were used in the calculation. This approach was chosen because a clear onset of densification, which could have served as the value for the ideal absorber, was not observed in the stress-strain curves.

2.2.3.8. Materials recovery. An approximately 2 cm × 2 cm × 1 cm piece of the 63 wt% panel was taken and immersed in a beaker containing approximately 150 mL of water. The sample was stirred constantly for 4 h at RT. After that, the recovered textiles pieces were placed in a non-stick sheet, and the solution containing the adhesive was poured into a rectangular mold. Both materials were left for 72 h under vacuum at RT in an oven.

3. Results and discussion

3.1. Surface, structure and physical properties

3.1.1. Textiles' morphology

The effect of mechanical transformation on the textile's morphology was qualitative observed using OM and SEM. Fig. 3 shows the fabric, yarn, and fibers morphology after mechanical transformation.

Fig. 3a illustrates that the fabric, despite undergoing the mechanical transformation, retains its integrity with no significant damage. The continuous weave structure of the fabric remains clearly visible. Upon closer inspection, fibers pulled from the yarn and cut extremities can be observed (Fig. 3b). Fig. 3c presents the fibers with non-hollow structure. Their extremities exhibit a combination of morphologies due to cutting and tensile solicitation experienced during processing, characteristic of a ductile material (Hearle et al., 1998). The surface morphology of the textiles observed by SEM, both before and after mechanical transformation are presented in Fig. 4.

As shown in Fig. 4, the material exhibits no surface damage prior to processing. After processing, the structure of the material is preserved, regardless of its type, for example: the woven structure of the fabric and the twisting of the yarn. However, smearing fibers were identified in some areas on the surface of the processed textile, as shown in Fig. 5. The observed damage could potentially be attributed to excessive friction between the fabrics during processing.

3.1.2. Density and percentage of porosity

The thermal and mechanical properties of the composite depend on the effective combination of the materials during fabrication. Porosity in the bulk material may indicate structural defects, such as phase discontinuities, resulting from insufficient adhesive. Considering this, Fig. 6 shows the density and porosity as a function of the textile's weight content. The density was compared to the theoretical density of the composite (T_d), calculated based on Equation (5):

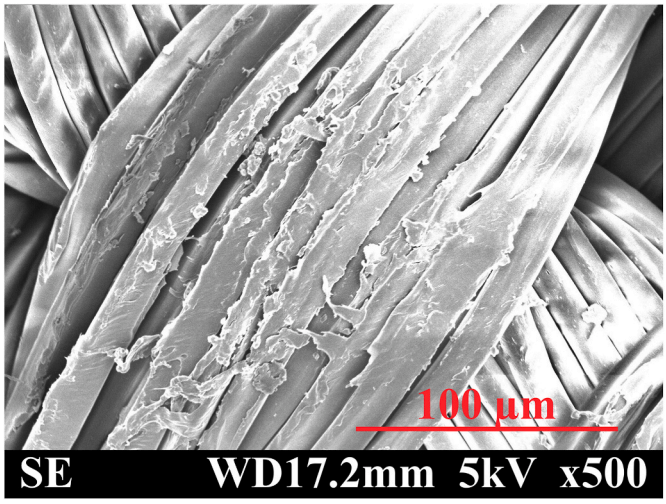

Fig. 5. Surface morphology of the fabric after processing.

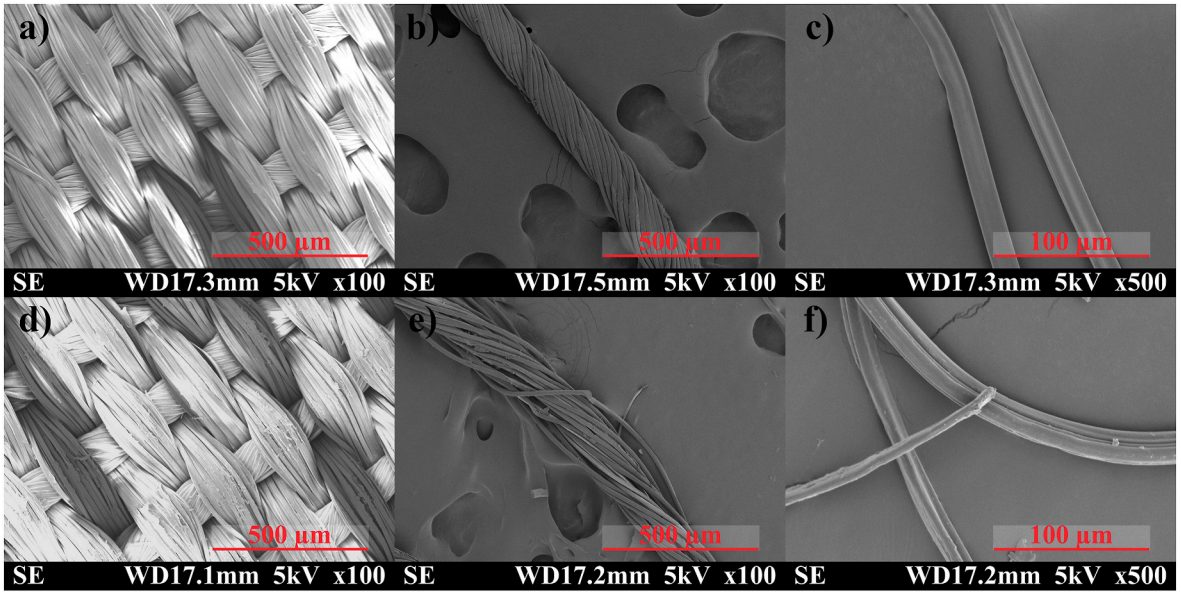

Fig. 4. Surface morphology of textile material before and after mechanical transformation: (a, b, c) fabric, yarn, and fiber before transformation, and (d, e, f) after transformation.

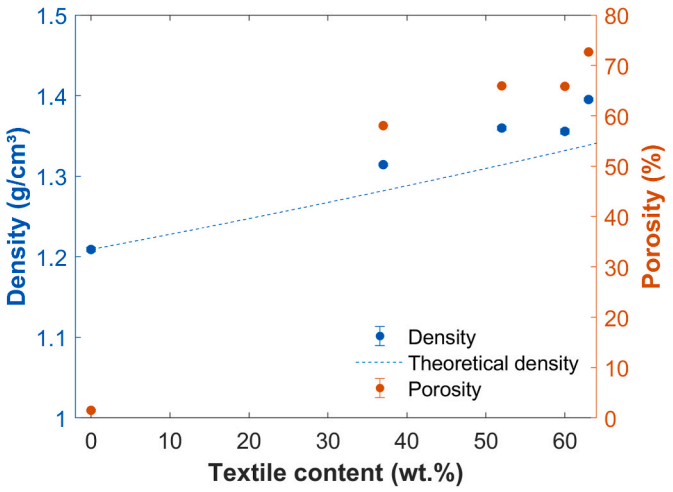

Fig. 6. Density and porosity as a function of the weight content of textile.

$$T_d = \frac{100}{\left(\frac{A_{wt\%}}{A_d} + \frac{R_{wt\%}}{R_d}\right)} \quad \text{Eq. 5}$$

where $A_{wt\%}$, $R_{wt\%}$, A_d, and R_d, represent the weight content and density of the adhesive and recycled textile, respectively. The R_d value was assumed as 1.428 g/cm^3 based on the measurement of the density of post-industrial recycled polyester fibers.

Considering the theoretical density (dashed line), a deviation from the measurements was observed and could be attributed to two factors. The first factor is the combination of different densities of the textile materials used in the composite. The second factor is the degree of porosity of the samples. As expect, porosity appears to be a function of the textile weight content, with a noticeable trend of increased porosity with higher textile content. For instance, a textile content of 37 wt% resulted in nearly 60 % porosity. The morphology of the adhesive and composites were investigated to better understand the porosity results.

3.1.3. Adhesive and composite morphology

Fig. 7 provides a comparison of the porosity morphology in the adhesive and composites with different textile contents.

The adhesive cross-section (Fig. 7a) exhibits porosity primarily as elliptical-shaped voids, highlighted in blue, with the longest sizes (major axis) ranging from 0.21 to 5.31 μm. However, with the addition of the textiles, regions of discontinuity between the matrix and textile are present, (Fig. 7b), although individual fibers are not apparent. At the maximum concentration of textile (Fig. 7c), the presence of dry spots (Patel and Lee, 1995) with individual fibers becomes more noticeable, and the spaces between them are insufficiently filled by the adhesive. This observation highlights the challenge of achieving optimal textile packing and adhesive wetting at higher textile concentrations at the same consolidation pressure, leading to increased porosity/voids and as later shown, negatively affecting the flexural behaviour of the samples. These challenges in wetting and fiber interaction are further exemplified by the water contact angle measurements, as the adhesive, being water-soluble, may interact less effectively with the textile surface.

3.1.4. Contact angle

Incorporating materials with different wetting properties might impact not only the composite's wettability and how it interacts with other adhesives or surface treatments in later processing stages but also how it interacts during the fabrication process. The average contact angle values for the adhesive, textile panel, and mechanically transformed textiles are depicted in Fig. 8. It also includes an example of the water droplets on the surface of these materials.

The adhesive's contact angle indicates its hydrophilic nature, with an average contact angle of approximately 65°. Incorporating textile material increased the surface roughness and enhanced the hydrophobicity, reaching a contact angle of 123° at a textile weight content of 63 %. This value matches the peak contact angle of 128° observed for polyester, which is expected as most of the composite surface is predominantly composed of textile material. The observed contact angle values highlight the differences in wetting behavior of the adhesive and textile surfaces, indicating increased difficulty for the adhesive to effectively flow and wet the textile during fabrication. As the textile content increases, the adhesive's ability to adequately wet the fibers becomes more challenging (Turner et al., 2024), leading to increased porosity and lack of bonding, as previously illustrated in Fig. 7c.

3.1.5. Thermal conductivity

The use of recycled textile material offers a promising alternative to

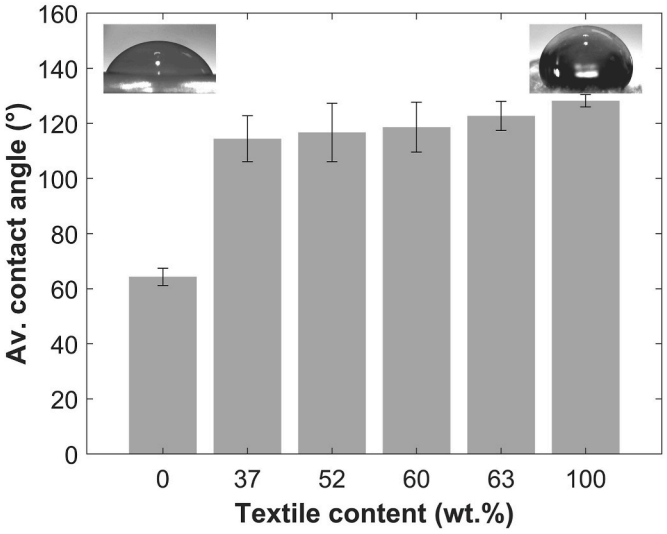

Fig. 8. Average contact angle of adhesive, textile panel and mechanically transformed textiles.

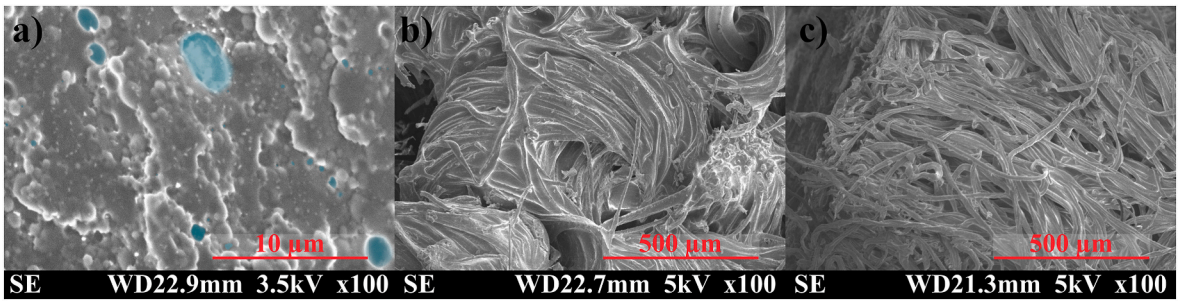

Fig. 7. a) Cross-section morphology of the adhesive, surface morphology of textile composite with b) 37 wt% and c) 63 wt%.

Table 2
Thermal conductivity of adhesive only and textile panels samples.

Textile content (wt.%)	Thermal Conductivity (W/m·K)	Density (g/cm^3)
0	0.3072 ± 0.0034	1.21 ± 0.01
37	0.0504 ± 0.0022	1.31 ± 0.01
52	0.0684 ± 0.0027	1.36 ± 0.01
60	0.0594 ± 0.0051	1.39 ± 0.01

conventional insulation solutions towards increased sustainability with adequate thermal performance. Table 2 summarizes the average thermal conductivity of the adhesive and composites.

The maximum reduction in thermal conductivity was observed with a six-fold reduction at a textile content of 37 wt%, compared to the sample containing only adhesive. However, any further increase in textile content beyond this concentration did not result in additional reductions in thermal conductivity. A similar result was published and was associated with the increased density of the composite (Valverde et al., 2013). Nonetheless, in the current study the addition of any amount of textile content resulted in a material that can be classified as a thermal insulator for building applications, as thermal conductivities less than 0.07 W/m·K were obtained (Asdrubali et al., 2015).

3.1.6. Acoustic response

The SAC and STL, presented in Fig. 9, are frequency-dependent indicators which respectively characterize the material's ability to absorb acoustic energy and block it from passing through. SAC values close to 0 indicate little to no sound absorption, while values near 1 represent complete sound absorption. In the case of STL, the higher the value, the better the panel's acoustic insulation.

As the textile content increases, Fig. 9a and b shows a global increase of the SAC. However, for rigid backed samples below 2000 Hz, the trend reverses, with the SAC slightly decreasing. Adding an air plenum significantly enhances the low-frequency SAC, as expected (Allard and Atalla, 2009) (see Fig. 9b), achieving values of 0.8 at 530 Hz and 3600 Hz for the material with 63 wt% textile content. The SAC difference between materials can be attributed to the increase in open porosity with higher textile content, which is associated with a reduction in airflow resistance of the samples (defined as the ratio of the pressure differential across a material sample to the normal flow through it; not measured in this study). An effective acoustic material for absorption applications requires a microstructure that allows fluid to flow through it, thereby enabling greater energy dissipation via viscous effects. However, this property also explains the observed decrease in STL with increasing textile content, as shown in Fig. 9c: porous materials with higher open porosity being less effective at blocking sound transmission.

To simplify the comparison between materials, single-value indicators were also calculated based on the frequency responses. In the case of the SAC, the frequency-averaged noise reduction coefficient (*NRC*) was calculated as the average sound absorption coefficient of the sample across four third-octave bands: 250 Hz, 500 Hz, 1000 Hz, and 2000 Hz. In the case of STL, the frequency-averaged sound transmission loss (STL_{avg}) was calculated as the average of the narrow band STL in the frequency band of interest. Table 3 summarizes the results.

Table 3
Summary of results of *NRC* and STL_{avg} of the textile panel samples.

Textile content (wt.%)	*NRC* - rigid backing (–)	*NRC* - 50 mm air plenum (–)	STL_{avg} (dB)
37	0.16 ± 0.01	0.23 ± 0.00	21.2 ± 0.0
52	0.15 ± 0.02	0.32 ± 0.02	17.6 ± 0.5
60	0.15 ± 0.02	0.39 ± 0.00	14.7 ± 0.1
63	0.13 ± 0.03	0.59 ± 0.01	9.8 ± 0.1

These single-value indicators accurately reflect the trends observed for the SAC of materials with an air cavity and the STL: the *NRC* increases while the STL_{avg} decreases with the textile content. However, it can be observed that the NRC in the rigid backing configuration slightly decreases with the increasing textile content in the material. This is due to the definition of the *NRC*, which only considers absorption values for frequencies below the upper limit of the one-third octave band at 2000 Hz. These results highlight the potential for designing textile sandwich panels that optimize both sound absorption and sound transmission loss by strategically varying the textile content across different layers of the composite structure for acoustic applications (Barbanera et al., 2020).

3.2. Mechanical properties

3.2.1. Three-point bending

Textile composites offer the advantage of combined properties, thereby broadening the range of potential applications. In addition to assessing the composites' thermal conductivity and acoustical behavior, the mechanical behavior of the textile-reinforced composites under flexural loading was investigated. Table 4 provides a summary of the results in terms of modulus of elasticity (E_B), maximum flexural stress (σ_f) and toughness.

Fig. 10 presents the a) flexural response in terms of stress and strain and b) the E_B as a function of samples's porosity percentage.

Samples based only on the adhesive exhibited a three times more rigid response compared to those with textiles, showing a higher E_B and σ_f. The addition of textiles increased the ductility of the samples, increasing the maximum supported strains. A similar trend was also reported for a composite based on poly(vinyl) alcohol and municipal solid waste (Ferrari et al., 2019). Despite a reduction in σ_f and E_B

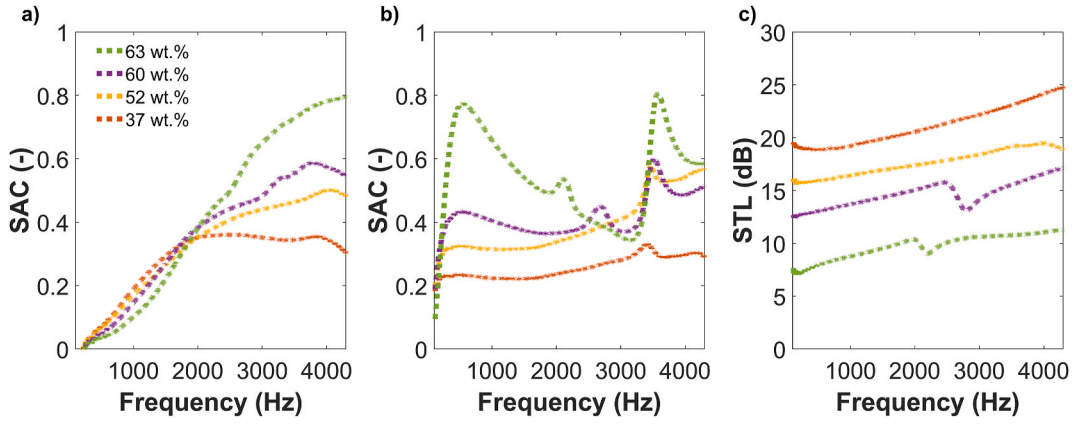

Fig. 9. Sound absorption coefficient (SAC) of the panels backed a) by a rigid termination; or b) backed by a 50 mm air plenum; and textile panels c) sound transmission loss (STL).

Table 4
Summary of results of E_B, σ_f, and toughness for adhesive and textile panel samples.

Textile content (wt.%)	E_B (MPa)	σ_f (MPa)	Toughness (kJ/m^3)
0	1273 ± 54	21 ± 4	189 ± 51
37	409 ± 49	13 ± 5	815 ± 141
52	183 ± 16	4 ± 1	406 ± 142
60	21 ± 6	2 ± 0	183 ± 59
63	10 ± 2	1 ± 0	98 ± 1

properties in all textile-based samples, an increase in toughness was obtained, increasing the energy required for fracturing. This represented a change from a brittle fracturing composite to a ductile one, with a larger plastic deformation, with the 37 wt% textile composites showing the highest toughness. The reduction in both E_B and σ_f might be related to the reduction of the overall amount of adhesive available for bonding the textile fibers leading to an increased percentage of porosity, as represented by Fig. 10b. A linear regression (LR) (dashed line) and the R-squared are presented to show the porosity and E_B association. The correlation was high ($R^2 = 0.97$), indicating a significant correlation between these two parameters. The results obtained are consistent with findings from investigations on conventional fiber-reinforced polymers, where void content played an important role in mechanical performance (Hagstrand et al., 2005), (SuhotC. and A., 2014). Although the materials differ, studies on glass fiber-reinforced polypropylene composites reported a reduction of approximately 1.5 % in E_B and σ_f for each 1 % increase in void content, indicating the negative effect of voids (Hagstrand et al., 2005). Based on this relationship, the porosity increase from around 2 %–58 % with the addition of 37 wt% textile content resulted in a 70 % reduction in E_B, which is in good agreement with an 84 % reduction approximated from the findings of the referenced study. This behavior, observed with increasing textile content, is likely influenced by the use of compression molding, a process that is prone to introducing greater porosity compared to other composite fabrication methods (Harris, 1999). To further assess the impact of reduced adhesive content on composite behavior, fracture surface analyses were conducted and are presented in Fig. 11.

Analysis of the fracture surfaces reveals a distinct difference in failure mechanisms at increased textile contents. At 37 wt% textile (Fig. 11a), it is possible to observe both adhesive-rich and textile-rich regions, indicating some degree of non-uniformity in the distribution, as well as the presence of voids. At higher magnification (Fig. 11b), fracture behavior appears to involve a combination of adhesive and cohesive failure. Good interfacial adhesion is evident from the presence of fiber breakage and limited fiber pull-out, indicating that the matrix can transfer the load to the textile fibers (Satapathy et al., 2008). Nonetheless, the surface of textile fibers does not appear to be coated with the adhesive, indicating lower compatibility between materials, as previously discussed. In contrast, the fracture surface at the highest textile content (Fig. 11c) exhibits extensive discontinuities and boundary regions. This lack of adhesive bonding and, critically, a reduction in the amount of matrix available to effectively wet and bond with the fibers limits stress transfer, leading to a noticeable decrease in mechanical performance. This is consistent with the observation that at higher fiber loadings, the matrix may not be sufficient to fully encapsulate and support the fibers, leading to increased porosity and reduced load transfer. The increased fiber-fiber interaction also contributes to this effect, as the fibers may interfere with each other's ability to effectively carry the load (Satapathy et al., 2008). Nonetheless, based on the σ_f results for composites with 37 wt% and 52 wt% textile content, these materials show potential for use as false ceiling boards in building applications (Zeleke and Rotich, 2021).

3.2.2. Impact testing

Given the increased toughness of the textile composites under flexural solicitations rather than increased strength, their shock absorption ability was investigated using the impact test method. Specifically, composites with 37 wt% and 52 wt% of textile materials were selected, as they showed the highest toughness compared to the neat material. Fig. 12 illustrates the samples behavior relative to the compressive

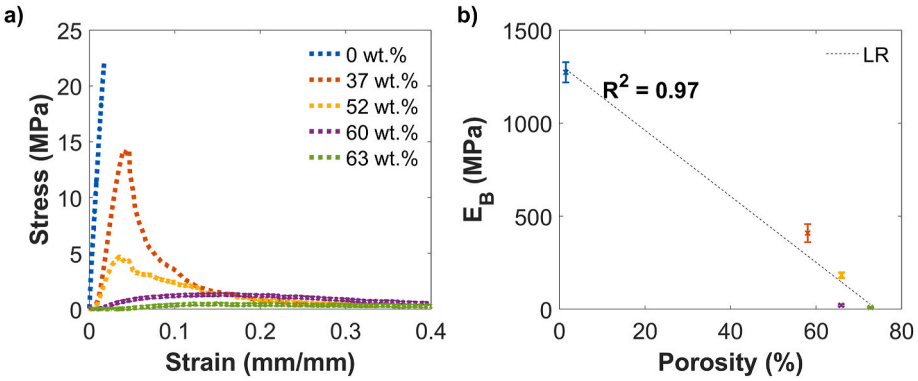

Fig. 10. a) Flexural response of adhesive and textile-panel samples, and b) modulus of elasticity (E_B) as a function of the sample's porosity.

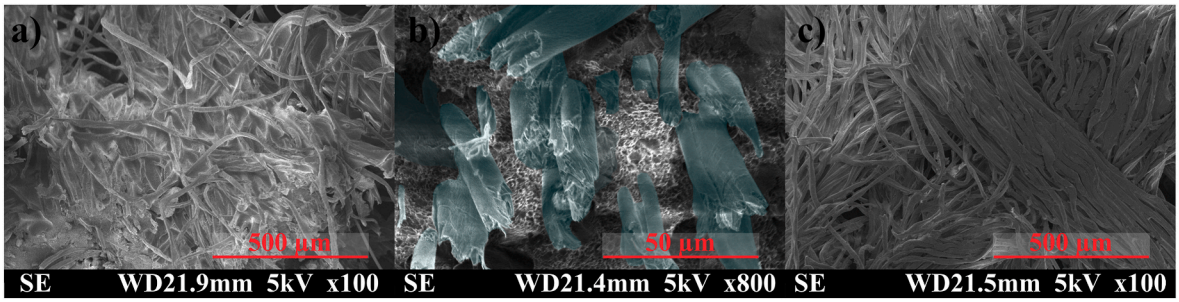

Fig. 11. Fracture surface of a textile composite with a) 37 wt% and its b) highlighted fibers at increased magnification, and at c) 63 wt%.

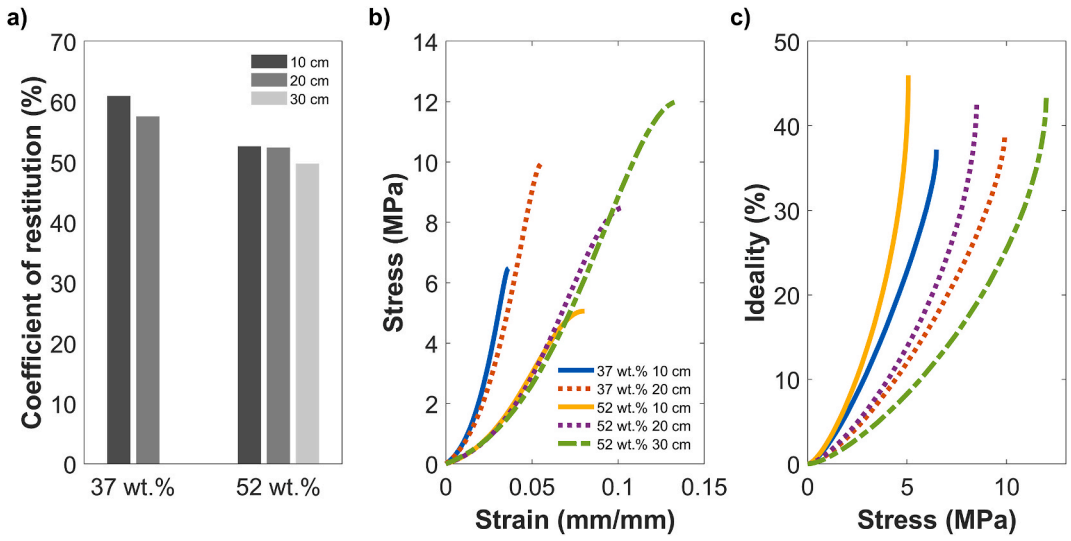

Fig. 12. a) Coefficient of restitution, b) compressive stress-strain response, and c) ideality as a function of stress of the composites.

solicitations shown by the a) coefficient of restitution, b) compressive stress-strain curve, and c) ideality.

Energy loss is indicated by lower COR values, opposed to a perfect elastic collision (COR of 100 %). As shown in Fig. 12a, higher drop heights resulted in a decrease in COR for both material compositions, indicating greater energy dissipation during impact. The 52 wt% composite samples exhibited lower COR values compared to the 37 wt% samples, suggesting enhanced energy absorption ability. Fig. 12b shows that the 52 wt% composites exhibited both larger deformations and enhanced toughness. At a drop height of 10 cm, the 52 wt% composite absorbed 117 % more energy compared to the 37 wt% composite. Interestingly, this is the opposite result of the flexural testing, where the combination of compressive and tensile solicitations resulted in lower toughness for those same compositions. Lastly, Fig. 12c shows that the 52 wt% composites displayed higher ideality values, indicating a greater capacity to approach the ideal behavior of an absorber for all tested heights.

3.3. Dissolution-based recycling

Recovering the starting materials is a key step towards increased recycling and reuse in the circular economy. Fig. 13 illustrates the recovery process of the 63 wt% composite.

As the figure illustrates, dissolution in water is an effective way to separate the water-soluble adhesive and the textile material, allowing their recovery. Following dissolution, the adhesive can be recovered by drying the water-based solution, yielding a film of the recovered material. This process highlights the potential for these materials to be recycled repeatedly, effectively contributing to a circular materials economy and reducing environmental impact. It should be noted that the performance and recyclability of the composite may be influenced by environmental factors, such as relative humidity or temperature. Changes in humidity could affect the adhesive properties, potentially reducing bonding strength and impacting overall material performance. On another note, the separation process was feasible due to the limited interaction between the materials, as indicated by the contact angle measurements. However, these results may vary depending on the textile composition. Textiles made of cotton or fiber blends may exhibit stronger interactions with the adhesive, which could hinder the efficiency of the separation and recovery process.

4. Conclusions and remarks

This study demonstrated the feasibility of fabricating recyclable textile-reinforced composites using a room-temperature processing method, emphasizing their potential for sustainable and circular economy applications. The incorporation of recycled textiles allowed tunable properties. Increased textile content enhanced sound absorption but reduced soundproofing due to higher porosity. While the fabrication process presented challenges, particularly with the amount of porosity introduced at higher textile content, the results highlight the versatility of these composites, which varied based on textile loading content. Additionally, the composites exhibited lower thermal conductivity, well-suited for thermal insulation applications for thermally efficient building applications. Furthermore, flexural toughness was highest at 37 wt% textile content, while impact toughness was greatest at 52 wt%,

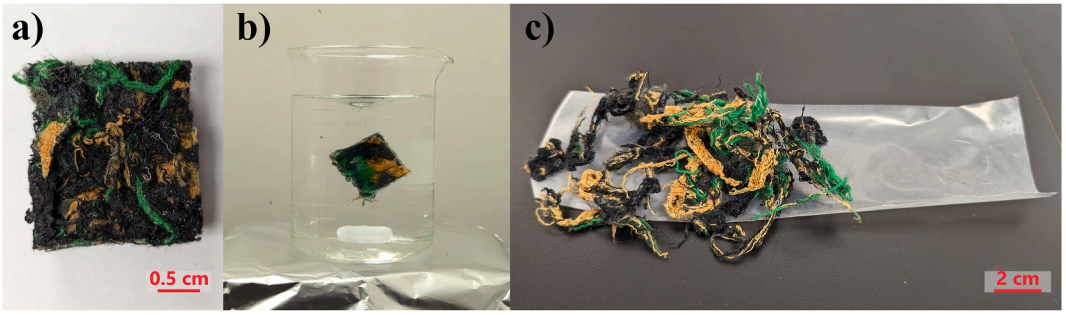

Fig. 13. Schematic of the water dissolution process for composite recycling, with a) the composite sample, b) dissolution process, and c) individual materials after dissolution and drying.

highlighting the materials' effectiveness in different energy absorption applications. Additionally, the ability to recover the materials using a water-based dissolution approach adds to the composites' feasibility within a circular economy framework, extending their lifespan.

Despite these findings, certain limitations should be acknowledged. First, only polyester-based post-industrial textile waste was used in this work. The behavior of composites incorporating other common textile materials or post-consumer textile waste was not investigated and may differ in terms of bonding, wetting behavior, or recyclability. Second, environmental testing was not conducted. Key aspects such as moisture resistance, biodegradability, thermal cycling and overall performance under environmental exposure were beyond the scope of this study and should be explored in future research.

The current findings offer a general framework for future research, which may be focused on three main directions: materials, process, and scalability. Future studies could explore different textile types (e.g., cotton-only and polyester-cotton blends) using the same adhesive system, to assess how fiber type influences final properties. On the process side, reducing porosity, especially at higher textile content, while maintaining room-temperature conditions will be essential to improve consistency and performance. Finally, once materials and processes are optimized, research into large-scale production methods and the scaling up of the water-based recovery process would be important steps toward making these composites both commercially viable and more sustainable. By addressing these areas, textile-based composites have the potential to result in low-impact materials for a wide range of indoor building applications including partitions, decorative panels, countertops, and furniture, contributing to a more circular and resource-efficient construction sector.

CRediT authorship contribution statement

José Carlos Ferreira Junior: Writing – original draft, Visualization, Validation, Methodology, Investigation, Formal analysis, Conceptualization. **Ennouri Triki:** Supervision, Methodology, Conceptualization. **Olivier Doutres:** Writing – review & editing, Methodology, Investigation. **Nicole R. Demarquette:** Writing – review & editing, Supervision. **Lucas A. Hof:** Writing – review & editing, Validation, Supervision, Project administration, Methodology, Funding acquisition, Conceptualization.

Funding

This work was supported by Mitacs through the Mitacs Accelerate program, École de technologie supérieure research funds, Centre interdisciplinaire de recherche en opérationnalisation du développement durable (CIRODD) via Levier program, and the City of Montreal, Quebec, Canada.

Declaration of competing interest

The authors declare that they have no known competing financial interests or personal relationships that could have appeared to influence the work reported in this paper.

Acknowledgements

The authors would like to acknowledge Serge Plamondon, Karim Kerkouche and Dorian Delbergue for their valuable help in collecting the experimental test data, three-point bending, impact testing and thermal conductivity, respectively. Our appreciation also goes to Adam St-Laurent (Vestechpro), for his support on the methodology and to both Adam St-Laurent and Bilel Letaief (Vestechpro) for their work in fabricating the panels. We are grateful to Renaissance Quebec for generously donating the post-industrial textiles. All these contributions were essential to the project.

Data availability

Data will be made available on request.

References

Algin, H.M., Turgut, P., 2008. Cotton and limestone powder wastes as brick material. Constr. Build. Mater. 22 (6), 1074–1080. https://doi.org/10.1016/j.conbuildmat.2007.03.006.

Allard, Jean F., Atalla, Noureddine, 2009. Acoustic impedance at normal incidence of fluids. Substitution of a fluid layer for a porous layer. In: Propagation of Sound in Porous Media: Modelling Sound Absorbing Materials, second ed. John Wiley & Sons Ltd, pp. 20–26.

Alshahrani, H., Ahmed, A., 2021. Enhancing impact energy absorption, flexural and crash performance properties of automotive composite laminates by adjusting the stacking sequences layup. Polymers 13 (19), 19. https://doi.org/10.3390/polym13193404.

Asdrubali, F., D'Alessandro, F., Schiavoni, S., 2015. A review of unconventional sustainable building insulation materials. Sustain. Mater. Technol. 4, 1–17. https://doi.org/10.1016/j.susmat.2015.05.002.

ASTM E1050-19, 2019. Test Method for Impedance and Absorption of Acoustical Materials Using a Tube, Two Microphones and a Digital Frequency Analysis System. https://doi.org/10.1520/E1050-19.

ASTM E2611-09, 2009. Test Method for Measurement of Normal Incidence Sound Transmission of Acoustical Materials Based on the Transfer Matrix Method. https://doi.org/10.1520/E2611-09.

Bailly, N., Petit, Y., Desrosier, J.-M., Laperriere, O., Langlois, S., Wagnac, E., 2020. Strain rate dependent behavior of vinyl nitrile helmet foam in compression and combined compression and shear. Appl. Sci. 10 (22), 8286. https://doi.org/10.3390/app10228286.

Barbanera, M., et al., 2020. Recycled leather cutting waste-based boards: thermal, acoustic, hygrothermal and ignitability properties. J. Mater. Cycles Waste Manag. 22 (5), 1339–1351. https://doi.org/10.1007/s10163-020-01024-3.

Barbero-Barrera, M.M., Pombo, O., Navacerrada, M. de los Á., 2016. Textile fibre waste bindered with natural hydraulic lime. Compos. Part B Eng. 94, 26–33. https://doi.org/10.1016/j.compositesb.2016.03.013.

Bediako, J.K., Wei, W., Yun, Y.-S., 2016. Conversion of waste textile cellulose fibers into heavy metal adsorbents. J. Ind. Eng. Chem. 43, 61–68. https://doi.org/10.1016/j.jiec.2016.07.048.

Brewer, M.K., 2019. Slow fashion in a fast fashion world: promoting sustainability and responsibility. Laws 8 (4), 4. https://doi.org/10.3390/laws8040024.

Briga-Sá, A., et al., 2013. Textile waste as an alternative thermal insulation building material solution. Constr. Build. Mater. 38, 155–160. https://doi.org/10.1016/j.conbuildmat.2012.08.037.

Broda, J., et al., 2019. Utilisation of textile wastes for the production of geotextiles designed for erosion protection. J. Text. Inst. 110 (3), 435–444. https://doi.org/10.1080/00405000.2018.1486684.

Bukhari, M.A., Carrasco-Gallego, R., Ponce-Cueto, E., 2018. Developing a national programme for textiles and clothing recovery. Waste Manag. Res. J. Sustain. Circ. Econ. 36 (4), 321–331. https://doi.org/10.1177/0734242X18759190.

Caro, F., Martínez-de-Albéniz, V., 2015. Fast fashion: business model overview and research opportunities. In: Agrawal, N., Smith, S.A. (Eds.), Retail Supply Chain Management: Quantitative Models and Empirical Studies. Springer US, Boston, MA, pp. 237–264. https://doi.org/10.1007/978-1-4899-7562-1_9. International Series in Operations Research & Management Science.

Casais, B., Faria, J., 2022. The intention-behavior gap in ethical consumption: mediators, moderators and consumer profiles based on ethical priorities. J. Macromarketing 42 (1), 100–113. https://doi.org/10.1177/02761467211054836.

Chen, Y., Wu, X., Wei, J., Wu, H., Fang, J., 2021. Reuse polyester/cotton blend fabrics to prepare fiber reinforced composite: fabrication, characterization, and interfacial properties evaluation. Polym. Compos. 42 (1), 141–152. https://doi.org/10.1002/pc.25814.

Delbari, S.A., Hof, L.A., 2024. Glass waste circular economy - advancing to high-value glass sheets recovery using industry 4.0 and 5.0 technologies. J. Clean. Prod. 462, 142629. https://doi.org/10.1016/j.jclepro.2024.142629.

Delpla, V., Kenné, J.-P., Hof, L.A., 2022. Circular manufacturing 4.0: towards internet of things embedded closed-loop supply chains. Int. J. Adv. Manuf. Technol. 118 (9–10), 3241–3264. https://doi.org/10.1007/s00170-021-08058-3.

DeVallance, D.B., Gray, J., Lentz, H., 2012. Properties of wood/recycled textile composite panels. Wood Fiber Sci. 44.

Dissanayake, D.G.K., Weerasinghe, D.U., Wijesinghe, K.A.P., Kalpage, K.M.D.M.P., 2018. Developing a compression moulded thermal insulation panel using postindustrial textile waste. Waste Manag. 79, 356–361. https://doi.org/10.1016/j.wasman.2018.08.001.

Drennan, K., Weber, S., Jacob-Vaillancourt, C., Kozlowski, A., Fiset-Sauvageau, L., Fashion Takes Action, 2021. A Feasibility Study of Textile Recycling in Canada.

Dris, R., Gasperi, J., Saad, M., Mirande, C., Tassin, B., 2016. Synthetic fibers in atmospheric fallout: a source of microplastics in the environment? Mar. Pollut. Bull. 104 (1–2), 290–293. https://doi.org/10.1016/j.marpolbul.2016.01.006.

Echeverria, C.A., Handoko, W., Pahlevani, F., Sahajwalla, V., 2019. Cascading use of textile waste for the advancement of fibre reinforced composites for building applications. J. Clean. Prod. 208, 1524–1536. https://doi.org/10.1016/j.jclepro.2018.10.227.

Egan, J., Salmon, S., 2022. Strategies and progress in synthetic textile fiber biodegradability. SN Appl. Sci. 4 (1), 22. https://doi.org/10.1007/s42452-021-04851-7.

Ellen MacArthur Foundation, 2017. A New Textiles Economy: Redesigning Fashion's Future. Ellen MacArthur Foundation [Online]. Available: http://www.ellenmacarthurfoundation.org/publications.

Farrant, L., Olsen, S.I., Wangel, A., 2010. Environmental benefits from reusing clothes. Int. J. Life Cycle Assess. 15 (7), 726–736. https://doi.org/10.1007/s11367-010-0197-y.

Fernandes, P.R.B., Contin, B., Siqueira, M.U., Ruschel-Soares, R., Baruque-Ramos, J., 2021. Biocomposites from cotton denim waste for footwear components. Mater. Circ. Econ. 3 (1), 29. https://doi.org/10.1007/s42824-021-00045-z.

Ferrari, F., Striani, R., Esposito Corcione, C., Greco, A., 2019. Valorization of food industries wastes for the production of poly(vinyl) alcohol (PVA) biodegradable composites. Front. Mater. 6, 177. https://doi.org/10.3389/fmats.2019.00177. Jul.

Frydrych, I., Ahmad, S., Umair, M., Shaker, K., Nawab, Y., Karahan, M., 2018. Mechanical behaviour of hybrid composites developed from textile waste. Fibres Text. East. Eur. 26 (1), 46–52. https://doi.org/10.5604/01.3001.0010.7796, 127.

Hagstrand, P.-O., Bonjour, F., Månson, J.-A.E., 2005. The influence of void content on the structural flexural performance of unidirectional glass fibre reinforced polypropylene composites. Compos. Part Appl. Sci. Manuf. 36 (5), 705–714. https://doi.org/10.1016/j.compositesa.2004.03.007.

Harris, B., 1999. 2.4 defects in manufactured polymeric composites. In: Engineering Composite Materials, second ed. Maney Publishing for IOM3, the Institute of Materials, Minerals and Mining, pp. 31–35 [Online]. Available: https://app.knovel.com/hotlink/pdf/id:kt00AVP15A/engineering-composite/defects-in-manufactured.

Hearle, J.W.S., Lomas, B., Cooke, W.D., 1998. 20. Other forms of severance. In: Atlas of Fibre Fracture and Damage to Textiles, second ed. Woodhead Publishing [Online]. Available: https://app.knovel.com/hotlink/pdf/id:kt003K9PM1/atlas-fibre-fracture/other-forms-severance.

Huang, Z., et al., 2024. A triple-crosslinking strategy for high-performance regenerated cellulose fibers derived from waste cotton textiles. Int. J. Biol. Macromol. 264, 130779. https://doi.org/10.1016/j.ijbiomac.2024.130779.

Juanga-Labayen, J.P., Labayen, I.V., Yuan, Q., 2022. A review on textile recycling practices and challenges. Textiles 2 (1), 174–188. https://doi.org/10.3390/textiles2010010.

Kunlere, I.O., Shah, K.U., 2023. A recycling technology selection framework for evaluating the effectiveness of plastic recycling technologies for circular economy advancement. Circ. Econ. 2 (4), 100066. https://doi.org/10.1016/j.cec.2023.100066.

Lacoste, C., El Hage, R., Bergeret, A., Corn, S., Lacroix, P., 2018. Sodium alginate adhesives as binders in wood fibers/textile waste fibers biocomposites for building insulation. Carbohydr. Polym. 184, 1–8. https://doi.org/10.1016/j.carbpol.2017.12.019.

Leal Filho, W., et al., 2022. An overview of the contribution of the textiles sector to climate change. Front. Environ. Sci. 10 [Online]. Available: https://www.frontiersin.org/articles/10.3389/fenvs.2022.973102. (Accessed 23 August 2023).

Mandarić, D., Hunjet, A., Vuković, D., 2022. The impact of fashion brand sustainability on consumer purchasing decisions. J. Risk Financ. Manag. 15 (4), 4. https://doi.org/10.3390/jrfm15040176.

Miltz, J., Ramon, O., 1990. Energy absorption characteristics of polymeric foams used as cushioning materials. Polym. Eng. Sci. 30 (2), 129–133. https://doi.org/10.1002/pen.760300210.

Mishra, R., Behera, B., Militky, J., 2014. Recycling of textile waste into green composites: performance characterization. Polym. Compos. 35 (10), 1960–1967. https://doi.org/10.1002/pc.22855.

Nayak, R., et al., 2020. Sustainable reuse of fashion waste as flame-retardant mattress filing with ecofriendly chemicals. J. Clean. Prod. 251, 119620. https://doi.org/10.1016/j.jclepro.2019.119620.

Nayanathara Thathsarani Pilapitiya, P.G.C., Ratnayake, A.S., 2024. The world of plastic waste: a review. Clean. Mater. 11, 100220. https://doi.org/10.1016/j.clema.2024.100220.

Niinimäki, K., Peters, G., Dahlbo, H., Perry, P., Rissanen, T., Gwilt, A., 2020. The environmental price of fast fashion. Nat. Rev. Earth Environ. 1 (4), 189–200. https://doi.org/10.1038/s43017-020-0039-9.

Nørup, N., Pihl, K., Damgaard, A., Scheutz, C., 2018. Development and testing of a sorting and quality assessment method for textile waste. Waste Manag. 79, 8–21. https://doi.org/10.1016/j.wasman.2018.07.008.

Nørup, N., Pihl, K., Damgaard, A., Scheutz, C., 2019. Quantity and quality of clothing and household textiles in the Danish household waste. Waste Manag. 87, 454–463. https://doi.org/10.1016/j.wasman.2019.02.020.

Pajunen, N., Rintala, L., Aromaa, J., Heiskanen, K., 2016. Recycling – the importance of understanding the complexity of the issue. Int. J. Sustain. Eng. 9 (2), 93–106. https://doi.org/10.1080/19397038.2015.1069416.

Patel, N., Lee, L.J., 1995. Effects of fiber mat architecture on void formation and removal in liquid composite molding. Polym. Compos. 16 (5), 386–399. https://doi.org/10.1002/pc.750160507.

Patnaik, A., Mvubu, M., Muniyasamy, S., Botha, A., Anandjiwala, R.D., 2015. Thermal and sound insulation materials from waste wool and recycled polyester fibers and their biodegradation studies. Energy Build. 92, 161–169. https://doi.org/10.1016/j.enbuild.2015.01.056.

Pegoretti, T. dos S., Mathieux, F., Evrard, D., Brissaud, D., Arruda, J.R. de F., 2014. Use of recycled natural fibres in industrial products: a comparative LCA case study on Acoustic components in the Brazilian automotive sector. Resour. Conserv. Recycl. 84, 1–14. https://doi.org/10.1016/j.resconrec.2013.12.010.

Peña-Pichardo, P., Martínez-Barrera, G., Martínez-López, M., Ureña-Núñez, F., dos Reis, J.M.L., 2018. Recovery of cotton fibers from waste blue-jeans and its use in polyester concrete. Constr. Build. Mater. 177, 409–416. https://doi.org/10.1016/j.conbuildmat.2018.05.137.

Petrucci, R., et al., 2015. Tensile and fatigue characterisation of textile cotton waste/polypropylene laminates. Compos. Part B Eng. 81, 84–90. https://doi.org/10.1016/j.compositesb.2015.07.005.

Rahman, S.S., Siddiqua, S., Cherian, C., 2021. Sustainability Assessment of Assorted Textile Waste as Reinforcement in wood-ash Treated Soil: an Expansion in the Horizon of Circular Textile Economy.

Ramamoorthy, S.K., Persson, A., Skrifvars, M., 2014. Reusing textile waste as reinforcements in composites. J. Appl. Polym. Sci. 131 (17). https://doi.org/10.1002/app.40687 n/a-n/a.

Ramamoorthy, S.K., Skrifvars, M., Alagar, R., Akhtar, N., 2018. End-of-life textiles as reinforcements in biocomposites. J. Polym. Environ. 26 (2), 487–498. https://doi.org/10.1007/s10924-017-0965-x.

Sadrolodabaee, P., Claramunt, J., Ardanuy, M., de la Fuente, A., 2021a. Characterization of a textile waste nonwoven fabric reinforced cement composite for non-structural building components. Constr. Build. Mater. 276, 122179. https://doi.org/10.1016/j.conbuildmat.2020.122179.

Sadrolodabaee, P., Claramunt, J., Ardanuy, M., de la Fuente, A., 2021b. Mechanical and durability characterization of a new textile waste micro-fiber reinforced cement composite for building applications. Case Stud. Constr. Mater. 14, e00492. https://doi.org/10.1016/j.cscm.2021.e00492.

Sadrolodabaee, P., Claramunt, J., Ardanuy, M., de la Fuente, A., 2021c. A textile waste fiber-reinforced cement composite: Comparison between short random fiber and textile reinforcement. Materials 14 (13), 3742. https://doi.org/10.3390/ma14133742.

Salissou, Y., Panneton, R., Doutres, O., 2012. Complement to standard method for measuring normal incidence sound transmission loss with three microphones. J. Acoust. Soc. Am. 131 (3), EL216–EL222. https://doi.org/10.1121/1.3681016.

Sandin, G., Peters, G.M., 2018. Environmental impact of textile reuse and recycling – a review. J. Clean. Prod. 184, 353–365. https://doi.org/10.1016/j.jclepro.2018.02.266.

Satapathy, S., Bihari Nando, Golok, Jose, J., Nag, A., 2008. Mechanical properties and fracture behavior of short PET fiber-waste polyethylene composites. J. Reinforc. Plast. Compos. 27 (9), 967–984. https://doi.org/10.1177/0731684407086626.

Shirvanimoghaddam, K., Motamed, B., Ramakrishna, S., Naebe, M., 2020. Death by waste: fashion and textile circular economy case. Sci. Total Environ. 718, 137317. https://doi.org/10.1016/j.scitotenv.2020.137317.

Suhot, M.A., C.A, R., 2014. The effects of voids on the flexural properties and failure mechanisms of carbon/epoxy composites. J. Teknol. 71 (2). https://doi.org/10.11113/jt.v71.3736.

Temmink, R., Baghaei, B., Skrifvars, M., 2018. Development of biocomposites from denim waste and thermoset bio-resins for structural applications. Compos. Part Appl. Sci. Manuf. 106, 59–69. https://doi.org/10.1016/j.compositesa.2017.12.011.

Turner, J., Lippert, D., Seo, D., Grasinger, M., George, A., 2024. Effect of wettability on the void formation during liquid infusion into fibers. Polym. Compos. 45 (16), 14931–14942. https://doi.org/10.1002/pc.28811.

Valverde, I.C., Castilla, L.H., Nuñez, D.F., Rodriguez-Senín, E., De La Mano Ferreira, R., 2013. Development of new insulation panels based on textile recycled fibers. Waste Biomass Valorizat. 4 (1), 139–146. https://doi.org/10.1007/s12649-012-9124-8.

Wang, Y., 1999. Utilization of recycled carpet waste fibers for reinforcement of concrete and soil. Polym.-Plast. Technol. Eng. 38 (3), 533–546. https://doi.org/10.1080/03602559909351598.

Yalcin-Enis, I., Kucukali-Ozturk, M., Sezgin, H., 2019. Risks and management of textile waste. In: Gothandam, K.M., Ranjan, S., Dasgupta, N., Lichtfouse, E. (Eds.), Nanoscience and Biotechnology for Environmental Applications, Environmental Chemistry for a Sustainable World, vol. 22. Cham: Springer International Publishing, pp. 29–53. https://doi.org/10.1007/978-3-319-97922-9_2, 22.

Yang, S., Song, Y., Tong, S., 2017. Sustainable retailing in the fashion industry: a systematic literature review. Sustainability 9 (7), 7. https://doi.org/10.3390/su9071266.

Zeleke, Y., Rotich, G.K., 2021. Design and development of false ceiling board using polyvinyl acetate (PVAc) composite reinforced with false banana fibres and filled with sawdust. Int. J. Polym. Sci. 2021, 1–10. https://doi.org/10.1155/2021/5542329.